THE JOURNAL OF BIOLOGICAL CHEMISTRY VOL. 290, NO. 9, pp. 5797–5809, February 27, 2015

Substituting Threonine 187 with Alanine in p27Kip1 Prevents Pituitary Tumorigenesis by Two-Hit Loss of *Rb1* and Enhances Humoral Immunity in Old Age*

Received for publication, November 10, 2014, and in revised form, January 11, 2015 Published, JBC Papers in Press, January 12, 2015, DOI 10.1074/jbc.M114.625350

Hongling Zhao[‡], Frederick Bauzon[‡], Enguang Bi[§], J. Jessica Yu[§], Hao Fu[‡], Zhonglei Lu[‡], Jinhua Cui[‡], Hyungjun Jeon[¶], Xingxing Zang[¶], B. Hilda Ye[§], and Liang Zhu[‡1]

From the [‡]Department of Developmental and Molecular Biology, and Medicine, and [§]Cell Biology, and [¶]Microbiology and Immunology, The Albert Einstein Comprehensive Cancer Center and Liver Research Center, Albert Einstein College of Medicine, Bronx, New York 10461

Background: p27T187A knockin mice facilitate studying p27Kip1 protein in physiology.
Results: p27T187A knockin prevented pituitary tumorigenesis in $Rb1^{+/-}$ mice and enhanced humoral response to immunization in older age.
Conclusion: Phosphorylation of p27T187 is important in *Rb1*-deficient tumorigenesis and immunity in aging.
Significance: Specific cancer is identified for treatment by inhibiting Skp2/Cks1-p27T187p interaction and new directions are revealed in understanding immunity decline in elderly.

p27Kip1 (p27) is an inhibitor of cyclin-dependent kinases. Inhibiting p27 protein degradation is an actively developing cancer therapy strategy. One focus has been to identify small molecule inhibitors to block recruitment of Thr-187-phosphorylated p27 (p27T187p) to $SCF^{Skp2/Cks1}$ ubiquitin ligase. Since phosphorylation of Thr-187 is required for this recruitment, p27T187A knockin (KI) mice were generated to determine the effects of systemically blocking interaction between p27 and Skp2/Cks1 on tumor susceptibility and other proliferation related mouse physiology. $Rb1^{+/-}$ mice develop pituitary tumors with full penetrance and the tumors are invariably $Rb1^{-/-}$, modeling tumorigenesis by two-hit loss of *RB1* in humans. Immunization induced humoral immunity depends on rapid B cell proliferation and clonal selection in germinal centers (GCs) and declines with age in mice and humans. Here, we show that p27T187A KI prevented pituitary tumorigenesis in $Rb1^{+/-}$ mice and corrected decline in humoral immunity in older mice following immunization with sheep red blood cells (SRBC). These findings reveal physiological contexts that depend on p27 ubiquitination by $SCF^{Skp2\text{-}Cks1}$ ubiquitin ligase and therefore help forecast clinical potentials of Skp2/Cks1-p27T187p interaction inhibitors. We further show that GC B cells and T cells use different mechanisms to regulate their p27 protein levels, and propose a T helper cell exhaustion model resembling that of stem cell exhaustion to understand decline in T cell-dependent humoral immunity in older age.

Cyclin-dependent kinase (Cdk)[2] inhibitor p27Kip1 (p27) binds cyclin/Cdk and inhibits their kinase activity. Since cyclin/Cdk drives the cell cycle engine, p27 and its family members p21 and p57 are best known as negative regulators of cell proliferation. p27 knock-out (KO) mice are larger and heavier by about 20% over wild type (WT) mice and develop pituitary intermediate lobe (IL) tumors, providing *in vivo* evidence for the anti-proliferative functions of p27 (1–3). p27 ck-mice [RxL32 to AxA32 knockin (KI) to disrupt p27 binding to cyclins, and FDF64 to ADA64 KI to disrupt p27 binding to Cdks] phenocopied p27 KO mice in larger body size and pituitary tumorigenesis, confirming the biochemical mechanisms of p27 function *in vivo* (4).

The best known mechanism for regulating p27 expression is its polyubiquitination leading to degradation in the proteasome, and the best known regulator of p27 ubiquitination is Skp2, which is the substrate recruiting subunit of the SCF^{Skp2} ubiquitin ligase (5). SCF^{Skp2} has a growing list of substrates. For recruiting p27, threonine 187 of p27 (p27T187) must be phosphorylated (6, 7) and an accessory protein, Cks1, must be present (8, 9). The phosphorylated threonine 187 fits into a pocket formed by Skp2 and Cks1 to enable stable interaction between p27 and Skp2/Cks1 (10); p27 is therefore ubiquitinated in the $SCF^{Skp2/Cks1}$-p27T187p complex.

p27T187A mutation (substitution of threonine with alanine) renders p27T187 unphosphorylable and, therefore, cannot be ubiquitinated by $SCF^{Skp2/Cks1}$. To test the biological significance of ubiquitination of p27T187p by $SCF^{Skp2/Cks1}$, p27T187A KI mice were generated (11).

Studies of cultured $p27^{T187A/T187A}$ mouse embryonic fibroblasts (MEFs) in serum starvation (to maintain MEFs in G0) and re-stimulation (to stimulate MEFs to proliferate) revealed re-

* This work was supported by NIH Grants R01CA127901and R01CA131421 (to L. Z.), and R01 CA85573 (to B. H. Y.). This work was also supported by a Department of Defense PCRP Postdoctoral Fellowship (PC121837) (to H. Z.), and the Irma T. Hirschl Career Scientist Award (to B. H. Y. and L. Z.).
[1] To whom correspondence should be addressed: Dept. of Developmental and Molecular Biology, Albert Einstein College of Medicine, 1300 Morris Park Ave., Room U-521, Bronx, NY 10461. Tel.: 718-430-3320; Fax: 718-430-8975; E-mail: liang.zhu@einstein.yu.edu.

[2] The abbreviations used are: Cdk, cyclin-dependent kinase; GC, germinal center; SRBC, sheep red blood cell; KI, knockin; KO, knock-out; MEF, mouse embryonic fibroblast; FACS, fluorescence-activated cell sorting; PNA, peanut agglutinin; IHC, immunohistochemistry; IF, immunofluorescence.

accumulation of p27 protein when cells entered S phase to levels seen in G0 phase, demonstrating that ubiquitination of p27T187p by $SCF^{Skp2/Cks1}$ is responsible for p27 protein degradation in S-G2 phases of the cell cycle (11). The biological effects of p27T187A KI varied with cell types. In MEFs stimulated by serum refeeding, p27T187A KI reduced S phase cell fraction by 20%. When splenic CD4+ T cells were activated by anti-TCR (T cell receptor), S phase cell reduction reached 80% (11). We will discuss the latter result further below.

At organismal level, since cells in adult tissues are mostly in quiescence, no abnormal p27 protein accumulation was detected in various tissues in $p27^{T187A/T187A}$ mice (11). $p27^{T187A/T187A}$ mice provide a gain-of-protein stability tool to study the effects of p27 protein accumulation in S-G2 of proliferating cells in physiological settings. For examples, Malek *et al.* (11) reported that healing of circular skin punch wounds was delayed by about 2-fold in $p27^{T187A/T187A}$ mice compared with WT mice when sizes of wounds were measured at 4.5 days after wounding. Proliferation of dermal keratinocytes around the wounds was reduced by 2.5 fold as measured by BrdU labeling. However, $p27^{T187A/T187A}$ mice grew larger than WT mice by about 20% in body weight at 80 days of age. Thus, p27T187A mutation produced proliferation-inhibitory as well as proliferation-stimulatory phenotypes. Mechanisms underlying the large body size phenotype of $p27^{T187A/T187A}$ mice remains to be determined.

Later studies examined $p27^{T187A/T187A}$ mice in other physiological processes involving cell proliferation, such as liver regeneration after partial hepatectomy (12), atherosclerosis and atheroma formation in ApoE KO mice on fat feeding (13), lung tumorigenesis following spontaneous activation of endogenous *Kras* (14), and multi-organ tumorigenesis following administration of carcinogen ENU to 15-day-old mice (14). Interestingly, in none of these experimental systems was p27T187A KI found to alter the main pathological/physiological outcomes. Only the ratios of histopathologically diagnosed carcinomas over adenomas were reduced in intestines of ENU-treated $p27^{T187A/T187A}$ mice compared with WT mice at necropsy (14).

At the same time, inhibitors of the Skp2/Cks1-p27T187p interaction are being actively developed as therapeutics for cancer (15–17) with the rationale that inhibiting this interaction would specifically stabilize p27 protein without affecting other substrates of SCF^{Skp2}, thereby minimizing side effects. $p27^{T187A/T187A}$ mice could model inhibitor treatment to block Skp2/Cks1-p27T187p interaction. Altogether, it is highly desirable and timely to define the type of cancers and normal physiological processes affected in $p27^{T187A/T187A}$ mice.

In this study, we examined the role of p27T187A KI in two experimental models. In the first, we crossed $p27^{T187A/T187A}$ mice with $Rb1^{+/-}$ mice to determine the effects of p27T187A KI on pituitary tumorigenesis in $Rb1^{+/-}$ mice, which models two hit loss of *RB1* in humans and is fully penetrant. Next, we tested $p27^{T187A/T187A}$ mice for T cell-dependent immunization response, which depends on B cell clonal expansion, diversification, and affinity selection within the germinal centers (GCs, (18)) in secondary lymphoid organs such as the spleen. We will describe these two experimental models in more details in relevant Results sections below.

EXPERIMENTAL PROCEDURES

Mice—$p27^{T187A/T187A}$ mice were described previously (11). Wild type and $p27^{T187A/T187A}$ mice were on mixed FVB and C57BL6J background. Mice were maintained under pathogen-free conditions in the Albert Einstein College of Medicine animal facility, and genotyped as previously described (19). Mouse experiments protocols were reviewed and approved by Einstein Animal Care and Use Committee, conforming to accepted standards of humane animal care.

Sheep Red Blood Cells (SRBC) Immunization—10–12-week-old mice (young mice) and 15–20-month-old mice (older mice) were immunized with 2×10^8 SRBC (Remel, R54012) by intraperitoneal injection. Spleens and sera were collected on day 10 for analyses.

Isolation of Splenocytes—Pieces of spleens were minced and passed through 70 μm cell strainers using the rod of 1 ml syringe into a 6-well plate in PBS. The strainers were washed with 1–2 ml of PBS. Cells were collected into a 15 ml tube and centrifuged at 1300 rpm for 5 min. Cell pellets were resuspended with 3–5 ml of red blood cell lysis buffer (155 mM NH_4Cl, 12 mM $NaHCO_3$, and 0.1 mM EDTA) and incubated at room temperature for 5 min. Then 10 ml of PBS+10%FCS was added to stop lysis, and splenocytes were collected by centrifugation.

Flow Cytometry (FACS)—5×10^6 to 1×10^7 isolated splenocytes were stained with fluorochrome-labeled antibodies at 4 °C for 30 min followed by washing with PBS/1% BSA, using our previously published protocol (20). Five-color flow cytometry was performed using an LSR II instrument (BD Biosciences) and the data were analyzed using FlowJo software (Tree Star, Inc.). At least 10,000 gated events were analyzed per mouse. For germinal center B cell analysis, isolated splenocytes were stained with DAPI (Sigma, D9564), Alexa 700-anti-B220 (BioLegend, 103231), FITC-PNA (Vector Labs, FL-1071), and PE anti-CD95 (Fas) (eBioscience, 12–0951-81). For T cell and B cell ratios analyses and CD4 and CD8 T cell ratios analyses, isolated splenocytes were stained with PE-anti-CD3 (BioLegend, 100205), Alexa 700-anti-B220 (BioLegend, 103231), Alexa 488-anti-CD4 (BioLegend,100425), and Alexa 647-anti-CD8a (BioLegend, 100727). Splenocytes were also stained with single fluorochrome-labeled antibody and used for compensation analyses.

Serum Anti-SRBC IgG ELISA—96 well EIA/RIA plates (Corning Inc., 9018) were coated for 1 h at 37 °C with either 100 μg/ml of SRBC ghosts prepared from sheep red blood cells (Thermo Fisher Scientific, R54012) for detecting antibodies in sera or mouse anti-goat IgG (H+L) (Southern Biotech, 1031-01) was used as plate coat to generate standard curve. The coated wells were blocked with 100 μl/well of 2% BSA/TBS for 1 h at 37 °C. Sera from unimmunized or immunized mice were serially diluted into 96 well plates in triplicate, and incubated overnight at 4 °C. After washed four times with TBST and bang dried, 96-well plates were added with 50 μl/well of alkaline phosphatase-labeled secondary antibody, goat anti-mouse IgG-AP (Southern Biotech, 1030-04), for 1 h at 37 °C. Alkaline

phosphatase substrate (0.5 mg/ml PNPP (Sigma, S0942)) in diethenolamine buffer (Fisher Scientific, 50-255-870) was then added to each well, and the plates were incubated 1 h at 25 °C before absorbance at 405 nm was measured in an ELISA reader. Serial dilutions and standard curves were performed to calculate antibody concentrations using Excel. Log transformation of concentrations was performed to obtain linear correlation between OD value and $\log_{10}$[concentration]. Purified isotype controls for mouse IgG1, IgG2a, IgG2b, and IgG3 (Southern Biotech) served as standards. Column scatter plots were generated by GraphPad Prism 6 software.

GC Number and Size Measurement—Overlapping images of entire spleen cross sections were reconstructed using "photomerge" (Adobe Photoshop CS3). Areas of entire spleen cross sections were used to determine GC numbers per mm^2. Sizes of individual GCs and spleen cross sections were measured in Image J. Column scatter plot of GC size was generated by GraphPad Prism 6 software; bar graph of GC numbers by Excel.

Tissue Sections and Staining—Pituitary glands and spleens were fixed in 10% formalin (Fisher Scientific, SF 100-4), embedded in paraffin wax and sectioned. For immunohistochemistry (IHC) and immunofluorescence (IF) staining, slides were deparaffinized, hydrated, and incubated in a steamer for 20 min in sodium citrate buffer (Vector Labs, H3301) for antigen retrieval. The following antibodies were used: anti-p27 (Abcam, ab92741), anti-CD3 (Santa Cruz Biotechnology, SC-20047), anti-B220 (BD Pharmingen, 550286), Ki67 (Vector Labs, SP6), anti-phosphorylated-Histon H3 (Cell Signaling Technology, #9701L), FITC-PNA (Vector labs, FL-1071), and Biotinylated PNA (Vector Labs, B-1075). SuperPicture™ kit (Invitrogen, 879263) and DAB kit with or without addition of nickel (Vector Labs, SK-4100) was used to detect p27 and Ki67 signals. Biotinylated anti-mouse (Vector Labs, BA-2000) and anti-rat (Vector Labs, BA-4000) antibodies were used as secondary antibodies for IHC CD3 and B220 staining, respectively, which were followed by Vectastain ABC kit (Vector Labs, PK-4004), and Red substrate kit (Vector Labs, SK-5100) for further red signal development. Biotinylated PNA was detected by Red substrate kit (Vector Labs, SK-5100). IF detection of pHH3, B220, CD3, and p27 was done by TSA™PLUS Fluorescence Kit (NEL741001KT, PerkinElmer), and PNA was by FITC-conjugated horse-anti-mouse-IgG (Vector Labs, FI-2000). DNA was stained with DAPI (Sigma, D9564). TUNEL staining was performed with an Apoptosis Detection Kit (Millipore, S7100).

Statistical Analysis—Four groups (young mice and older mice, each separated into WT and p27T187A KI genotypes) of data from ELISA and GC B cell FACS (Figs. 2 and 3, respectively) were analyzed by two-way (ages and genotypes) ANOVA (GraphPad Prism 6 Software), followed by unpaired two-tailed Student's *t* test (GraphPad Prism 6 Software) for pairs of WT and p27T187A in each age groups and pairs of young and older mice for each genotypes. Two groups (older WT and older p27T187A KI) of data from GC numbers and sizes measurements and pHH3 positive cell frequency in GC, and ratios of T/B cells and CD4+/CD8+ T cells (Figs. 4 and 7, respectively) were analyzed by unpaired two-tailed Student's *t* test (GraphPad Prism 6 Software). $p < 0.05$ is considered statistically significant.

RESULTS

p27T187A KI Prevents $Rb1^{+/-}$ Mice from Developing Pituitary Tumors—Study of retinoblastomas led to the identification of the prototype tumor suppressor pRb. Typical retinoblastoma patients inherit one null allele of *RB1* from one parent and therefore are $RB1^{+/-}$, they develop retinoblastoma with full penetrance and the tumors invariably are $RB1^{-/-}$. These characteristics led to the two-hit hypothesis for tumorigenesis by inactivation of a tumor suppressor. pRb is highly conserved in mouse (*Rb1* in mouse) and $Rb1^{+/-}$ mice develop melanotroph tumors in pituitary IL with full penetrance and the tumors are invariably $Rb1^{-/-}$ (21). We used this physiological setting to test $p27^{T187A/T187A}$ mice in oncogenic proliferation.

As expected, all ($n = 5$) $Rb1^{+/-}$ mice contained pituitary IL tumors when examined at 6 months of age. In comparison, all $Rb1^{+/-}$;$p27^{T187A/T187A}$ mice ($n = 5$) contained microscopically normal pituitary glands at 9 months of age, indistinguishable from pituitaries in wild type and $p27^{T187A/T187A}$ mice (Fig. 1*A*).

When measured by p27 IHC, expression of p27 in IL is low in WT, *Skp2* KO, and *POMC-Cre;*$Rb1^{lox/lox}$ (which deletes *Rb1* in all melanotrophs in IL) mice. Only when *Skp2* and *Trp53* were co-deleted in IL did p27 protein levels rise to produce robust staining, since co-deletion of *Skp2* and *Trp53* reduced the cellular pool of p27 ubiquitin ligases including Skp2, Pirh2, and KPC1 (22). Fig. 1*B* shows that p27 IHC produced similarly low staining in WT and $p27^{T187A/T187A}$ IL; tumors in $Rb1^{+/-}$ IL showed higher nuclear density but individual nuclei showed similar staining intensity with those in areas of normal IL; and $Rb1^{+/-}$;$p27^{T187A/T187A}$ IL was not different from $p27^{T187A/T187A}$ IL. In the same experiment, the IL of *POMC-Cre;*$Rb1^{lox/lox}$;*Trp53*$^{lox/lox}$;$Skp2^{-/-}$ mice showed robust staining (Fig. 1*C*).

These results document that blocking phosphorylation of p27T187 and, by extension, preventing p27 ubiquitination by $SCF^{Skp2/Cks1}$ does not result in overt accumulation of p27 protein in pituitary IL in adult mice, but can prevent pituitary IL tumorigenesis by two hit loss of *Rb1*.

$p27^{T187A/T187A}$ Mice Develop Normal T Cell-dependent Antibody Response that Does Not Decline with Age—Immunization with T cell dependent antigens, such as SRBC, induces robust antibody response that is largely dependent upon the formation of GCs in secondary lymphoid tissues (humoral immunity). The GC reaction is characterized by dramatic clonal expansion of GC B cells and selection of affinity matured subclones into either plasma cell or memory B cell pools. These dynamic changes in the GC B cell population are orchestrated by CD4+ follicular helper T cells (Tfh) in GC (23, 24). The GC response provides a physiological setting of robust but non-oncogenic proliferation to study cell cycle regulation (20, 25). In addition, both the magnitude and functional output of GC reaction decline in old age, a phenomenon contributing to increased incidence of vaccine-preventable diseases in the elderly population (26). We hypothesized that $p27^{T187A/T187A}$ mice, especially in older age, wound show impaired T cell-dependent antibody response, and set out to test our hypothesis.

In unimmunized mice, serum anti-SRBC IgG levels were at base levels in all test groups (Fig. 2*A*). We immunized 12-week-old WT and $p27^{T187A/T187A}$ mice (10–12-week-old mice will be

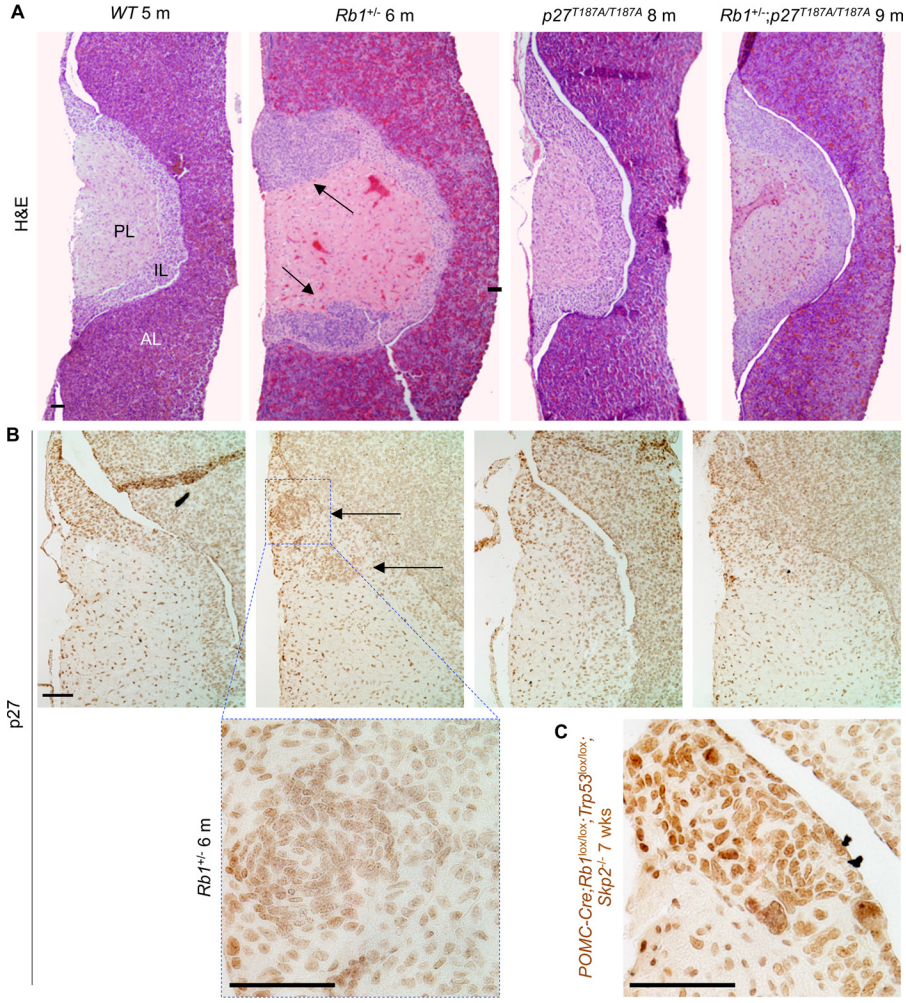

FIGURE 1. **Rb1$^{+/-}$;p27$^{T187A/T187A}$ mice do not develop pituitary tumors.** *A*, representative coronal sections of mouse pituitaries were stained with H&E. The three pituitary lobes are marked. *PL*, posterior lobe; *IL*, intermediate lobe; *AL*, anterior lobe. *Rb1*$^{+/-}$ mice at 6 months of age ($n = 5$) contained one to two IL tumors as marked by *black arrows*, while *Rb1*$^{+/-}$,*p27*$^{T187A/T187A}$ mice at 9 months of age ($n = 5$) contained pituitaries identical to those in WT and *p27*$^{T187A/T187A}$ mice. *B*, representative p27 IHC sections showing low level staining in WT, *Rb1*$^{+/-}$, *p27*$^{T187A/T187A}$, and *Rb1*$^{+/-}$;*p27*$^{T187A/T187A}$ IL, under the H&E images of the same genotypes. *C*, in the same experiment, *POMC-Cre;Rb1*$^{lox/lox}$;*Trp53*$^{lox/lox}$;*Skp2*$^{-/-}$ IL showed robust p27 staining. Scale bars, 100 μm.

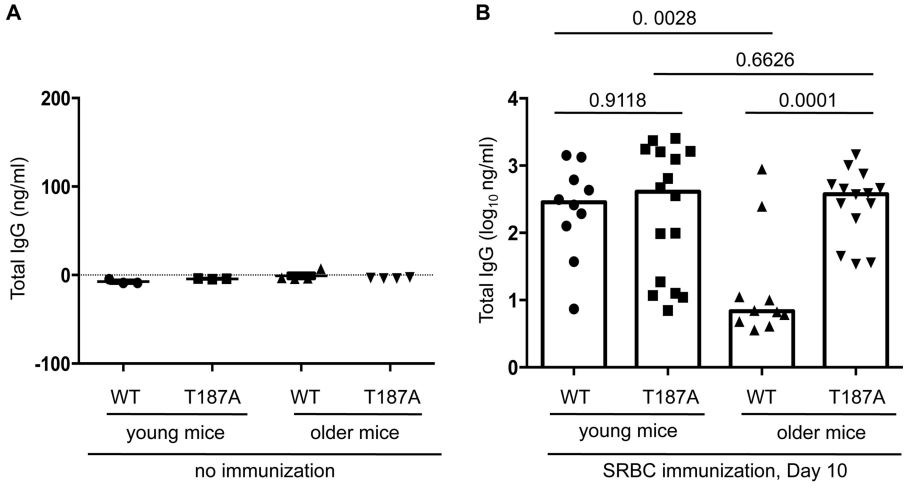

FIGURE 2. **Serum anti-SRBC IgG titers following SRBC immunization decline with age in WT but not *p27*$^{T187A/T187A}$ mice.** *A*, unimmunized WT or *p27*$^{T187A/T187A}$, young or older mice show similar base level serum anti-SRBC IgG titer. *B*, serum anti-SRBC IgG was measured 10 days after SRBC immunization. *WT* represents *p27*$^{+/+}$, *T187A* for *p27*$^{T187A/T187A}$. *young mice* were between 10 and 12 weeks old; *older mice* between 15 and 20 months old. Each data point represents one individual, and column heights show medians. Statistical analysis by two-way ANOVA with these four groups of data showed $p = 0.0129$ for differences between young and older, and $p = 0.0036$ for differences between WT and T187A. Unpaired two-tailed Student's *t* tests were used to determine *p* values between various pairs of samples as marked in the plot.

called "young mice") with SRBC and, on day 10, measured serum titers of anti-SRBC IgG. We found no significant differences between serum titers of anti-SRBC IgG in young WT and young $p27^{T187A/T187A}$ mice (Fig. 2*B*, *young mice*). Thus, p27T187A KI does not change the outcomes of SRBC immunization in young mice.

We went on to determine whether decline in humoral immunity would be greater in aging $p27^{T187A/T187A}$ mice than in aging WT mice. We found that anti-SRBC IgG titers reduced significantly in 15–20-month-old WT mice (15–20-month-old mice will be called "older mice") compared with young WT mice, but anti-SRBC titers in older $p27^{T187A/T187A}$ mice were not different from those in young $p27^{T187A/T187A}$ mice (Fig. 1*B*). As such, older $p27^{T187A/T187A}$ mice produced significantly higher titers of anti-SRBC IgG than older WT mice. Both two-way (ages and genotypes) ANOVA and Student's *t* test were performed for these analyses (see Fig. 2 legend). These findings proved opposite to our hypothesis, but phenotypically reveal that phosphorylation of p27T187 and, by extension, ubiquitination of p27 by $SCF^{Skp2/Cks1}$ promotes decline in humoral immunity in older mice.

Spleen GC Reactions Decline in Older WT, but Not Older $p27^{T187A/T187A}$, Mice—Antigen-specific antibody titers reflect the magnitude and quality of the GC response, in which naïve resting B cells convert to highly proliferating GC B cells. To determine the bases for the higher antibody titer in immunized older $p27^{T187A/T187A}$ mice, we determined how much B cell in total B cell population had converted to GC B cells at day 10 following SRBC immunization of four test groups of mice (as plotted in Fig. 3*D*). B cells are identified by B cell marker B220. GC B cells have additionally become positive for peanut agglutinin (PNA) affinity-staining and anti-Fas immune-staining. Spleen cell suspensions prepared on day 10 following SRBC injection were first gated on side and forward scatter to exclude aggregates and then for high B220 staining (for total B cells) and low DAPI staining (for total live B cells) (Fig. 3*A*). Within the total live B cell populations, GC B cell populations were identified as positive for both PNA and Fas. As shown in Fig. 3, *B* and *C*, and quantified in Fig. 3*D*, GC B cell populations ranged from 0.1% to 0.8% of the total B cell populations in non-immunized young and older, WT, and $p27^{T187A/T187A}$ mice. Following SRBC immunization GC B cell populations within total B cell populations increased in young WT and young $p27^{T187A/T187A}$ mice to 4.6% and 6.1%, respectively. With aging, GC B cell populations within total B cell populations declined in older WT mice (from 4.6% to 2.1%), but not in older $p27^{T187A/T187A}$ mice (from 6.1% to 6.3%). When older mice are compared, total B cell populations of older $p27^{T187A/T187A}$ mice contained significantly more GC B cells than older WT mice's total B cell populations. Both two-way (ages and genotypes) ANOVA and Student's *t* test were performed for the four groups of data (see Fig. 3*D* and its legend).

To directly visualize the GC structure, we stained spleen sections from immunized animals with PNA, and defined the PNA positive regions within the primary B cell follicles as GCs. p27T187A KI did not alter the spleen red pulp or white pulp morphology, nor did it cause spontaneous GCs in unimmunized animals of all age groups (not shown). After SRBC immunization, however, older $p27^{T187A/T187A}$ spleens developed many large GCs and often contained several GCs in each primary follicle compared with small to medium sized GCs each located within one follicle in the WT spleens (Fig. 4*A*). We quantified the GC density and size for individual spleen sections among the four experimental groups, and the results show that older $p27^{T187A/T187A}$ mice contained more numerous and larger GCs than older WT mice (Fig. 4, *B* and *C*). These results support the findings by FACS that GC B cell population sizes were larger in older $p27^{T187A/T187A}$ mice than in older WT mice (Fig. 3). A more robust GC reaction in older $p27^{T187A/T187A}$ mice could explain their improved anti-SRBC IgG titers relative to their WT counterparts.

We next examined the proliferation status of GC B cells using immune-staining for Ki67. Ki67 staining appeared similarly intense between older WT and young WT mice and between older WT and older $p27^{T187A/T187A}$ mice (Fig. 4*D* and data not shown). Although GCs in older WT mice are smaller than GCs in older $p27^{T187A/T187A}$ mice, nearly all PNA positive cells stained positive for Ki67 in both types of older mice (Fig. 4*D*). When GC B cells were stained with the mitotic marker phosphorylated histone H3 (pHH3), we found more pHH3 positive cells in GCs in older $p27^{T187A/T187A}$ mice than in older WT mice (Fig. 4, *E* and *F*), suggesting that more cell division could explain the larger GC B cell population sizes in older $p27^{T187A/T187A}$ mice. However, the increases did not reach statistical significance (Fig. 4*F*). TUNEL staining was similarly intense in older WT mice, young WT mice, and older $p27^{T187A/T187A}$ mice (data not shown). Thus, both the decline in older WT mice and the maintenance in older $p27^{T187A/T187A}$ mice of GC B cell population sizes were not correlated with dramatic decreases (in the decline in older WT mice) or increases (in the maintenance in older $p27^{T187A/T187A}$ mice) in Ki67 or pHH3 labeling of GC B cells.

In aggregate, by showing more robust production of GC B cells in older $p27^{T187A/T187A}$ mice than in older WT mice, results in this section explained improved serum titers of anti-SRBC IgG in older $p27^{T187A/T187A}$ mice. These findings however do not explain how p27T187A KI induced more robust GC B cell production.

p27 Expression Decreases When Naïve B Cells Are Recruited into GC in Both Older WT and Older $p27^{T187A/T187A}$ Mice—We next compared p27 expression in the spleens of older WT and older $p27^{T187A/T187A}$ mice at day 10 following SRBC injection, when the GC reactions were more robust in older $p27^{T187A/T187A}$ mice than in older WT mice.

In post-immunization spleens from both older WT and older $p27^{T187A/T187A}$ mice, the B220+ B cell area and CD3+ T cell zone occupy discrete areas in the white pulp (Fig. 5, *A*, *a*,*e* and *B*, *a*,*e*). The PNA+B220weak GCs were embraced by the PNA-B220+ primary B cell follicles from one side (Fig. 5*A*, *a*–*h*) with its other side likely facing the more discrete T cell zone (27, 28) (Fig. 5*B*, *a*–*h*).

Interestingly, the pattern of p27 staining is much broader than either the B220- or CD3-marked areas alone, suggesting that p27 is expressed in the majority of B and T cells outside of the GCs (also see below), and similar in older WT and older $p27^{T187A/T187A}$ spleen sections, suggesting that T187A KI did

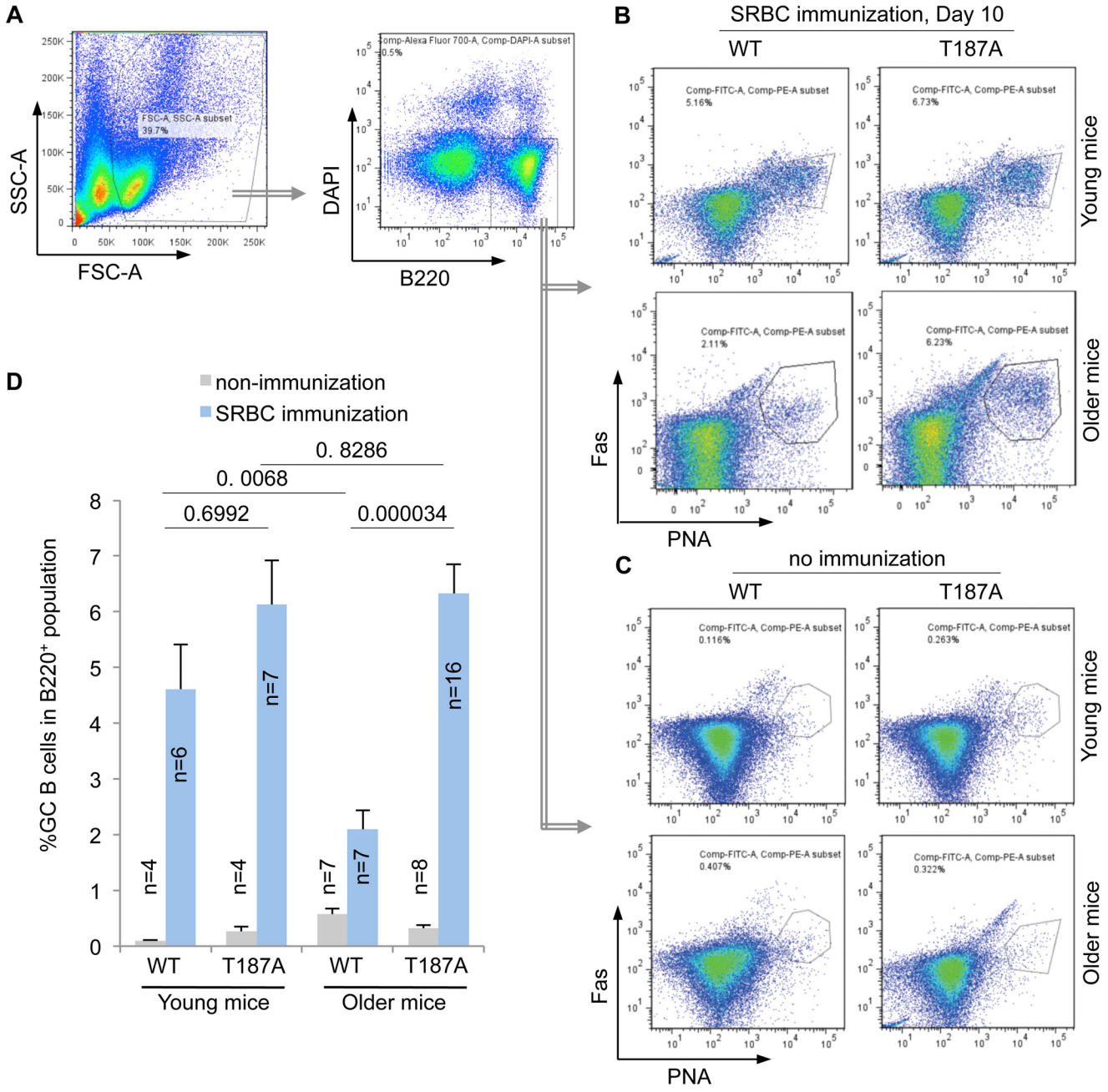

FIGURE 3. **Production of spleen GC B cells following SRBC immunization decline with age in WT but not *p27*$^{T187A/T187A}$ mice.** *A*, FACS of total spleen cell suspension, showing the first FSC-SSC gate, followed by the B220 and DAPI gate. DAPI^{low},B220^{high} cells then underwent FACS on PNA and Fas to determine population sizes of GC B cells (PNA^{high} and Fas^{high}) in total B cell population at day 10 following SRBC immunization (*B*) or from unimmunized mice (*C*). Quantifications of *B* and *C* are shown in *D*. Error bars represent S.E. Two-way ANOVA with these four groups of data from immunized mice showed $p = 0.0850$ for differences between young and older, and $p = 0.0001$ for differences between WT and T187A. Unpaired two-tailed Student's *t* tests were used to determine *p* values between various sample pairs as shown in *D*.

not induce notable p27 accumulation in *p27*$^{T187A/T187A}$ spleens (Fig. 5*C*, *a* and *e*). Notable however are round punctuates where p27 staining was dramatically reduced (*black arrows* in Fig. 5*C*, *a* and *e*) inside the broad and otherwise evenly stained p27+ areas in both WT and *p27*$^{T187A/T187A}$ spleens. Double immunofluorescence (IF) staining with PNA and anti-p27 demonstrate that the p27 low areas are populated by PNA+ GC B cells (*white arrows* in Fig. 5, *c*,*d* and *g*,*h*). High magnification images confirmed that the vast majority of PNA+ GC B cells are p27 negative irrespective of the p27 genotype (Fig. 6*A*). Thus, in the B cell lineage, p27 protein levels were dramatically down regulated when the naïve resting B cells (which populate the more intensely stained B220+ area) are recruited into the highly proliferative GCs regardless of the *p27*$^{T187A/T187A}$ mutation status.

Since GC B cells were actively proliferating in both older WT and older *p27*$^{T187A/T187A}$ mice (Fig. 4, *D* and *E*), the dramatic down-regulation of p27 in GC correlated with highly active proliferation of GC B cells. To identify mechanisms for this down-regulation in GC B cells, we determined whether p27 mRNA levels were down regulated in GC B cells. For this purpose, we searched NCBI databases for gene expression profile datasets that compared naïve resting B cells with GC B cells. We

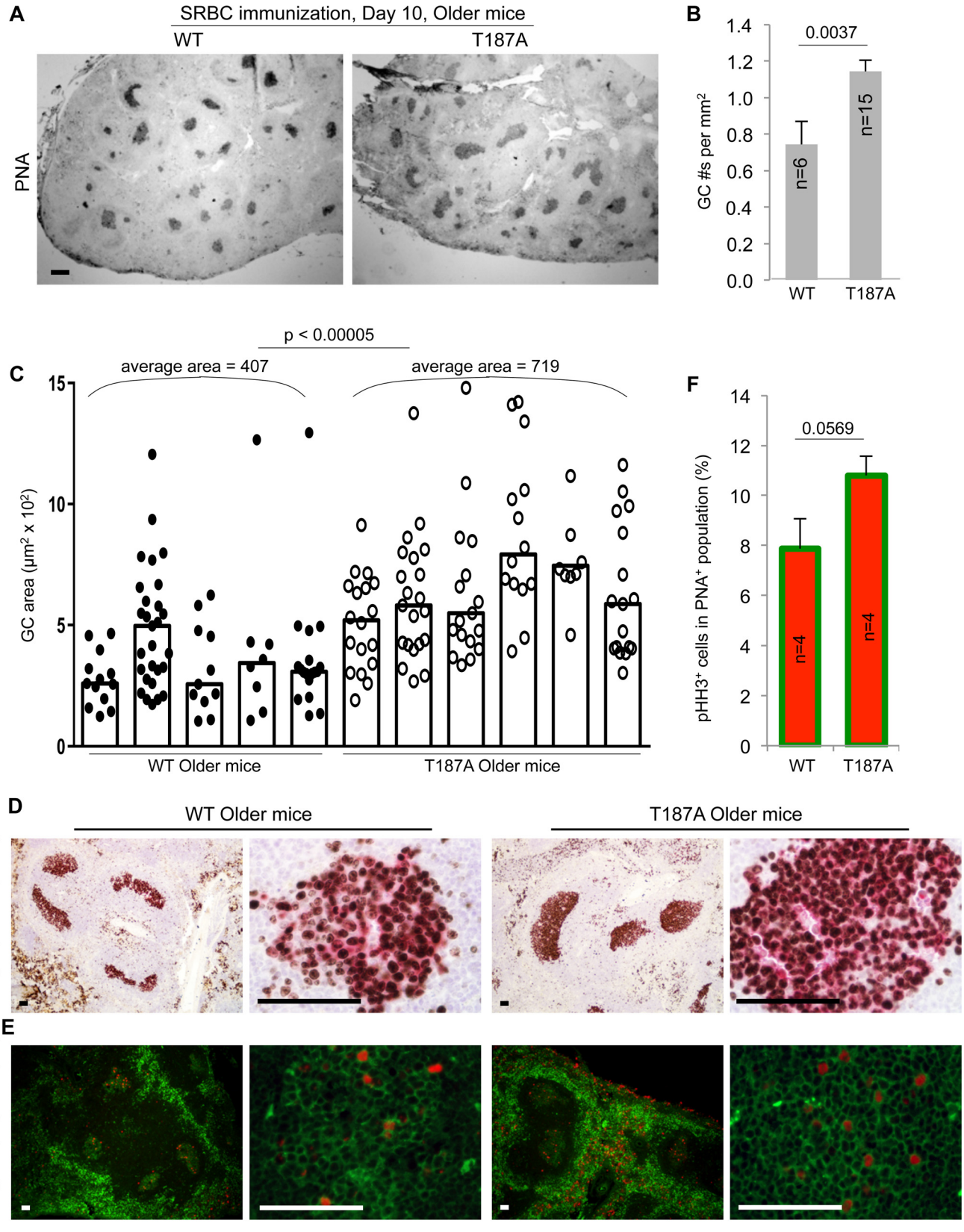

FIGURE 4. **Spleen GC numbers and sizes are higher and larger in older *p27*$^{T187A/T187A}$ mice than in older WT mice at 10 days following SRBC immunization.** *A*, representative images of spleen sections stained with PNA to visualize GC. Scale bars, 200 μm. *B*, quantifications of GC numbers on spleen sections, error bars are S.E. *C*, quantifications of GC sizes. Each column represents one individual, and each point is an individual GC. Column heights represent medians. Co-staining of Ki67 (*black*) and PNA (*red*) (*D*), and pHH3 (*red*) and PNA (*green*) (*E*), of GC were performed on spleen sections as marked. Scale bars, 50 μm. *F*, quantification of data in *E*. *p* values are from two-tailed Student's *t* tests.

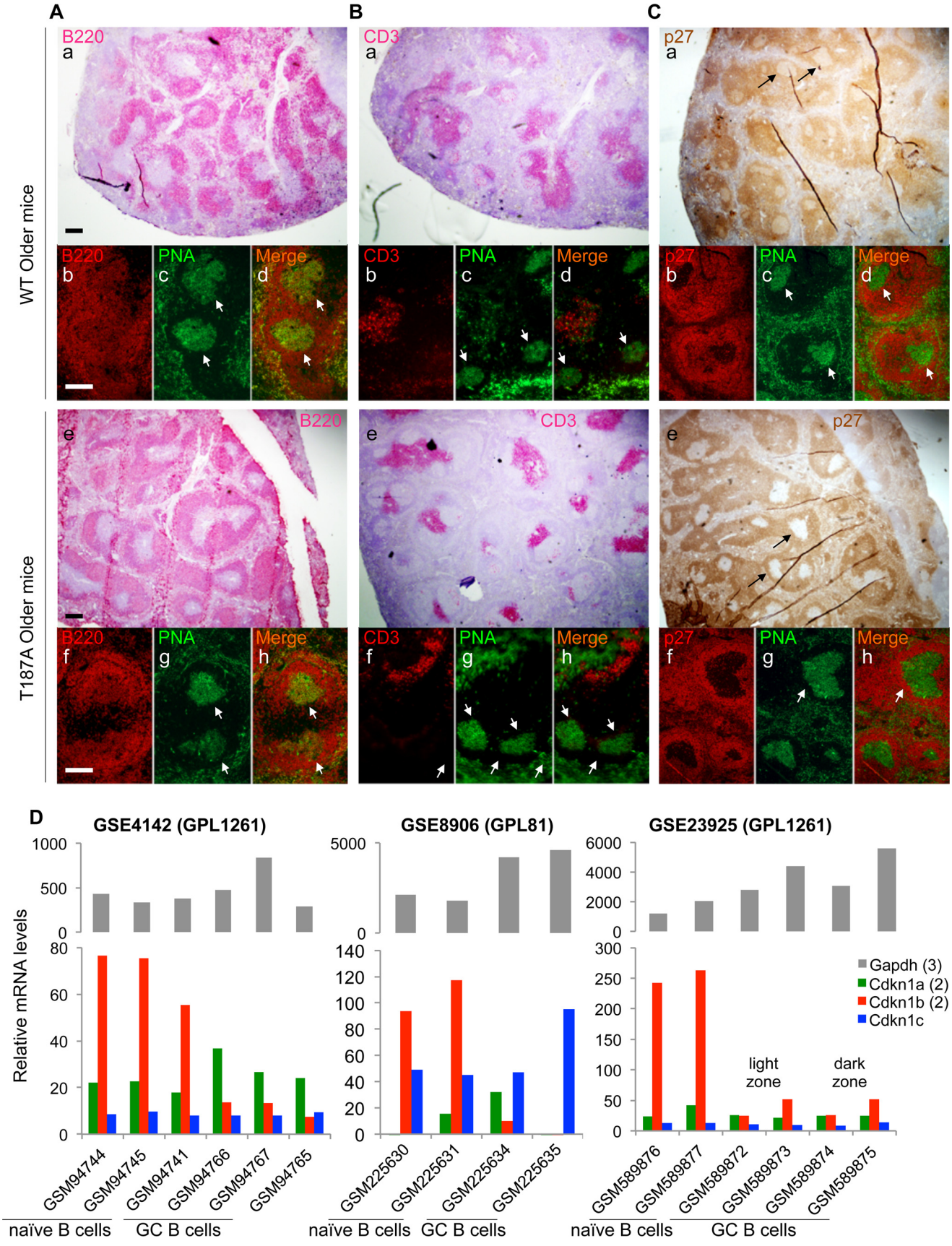

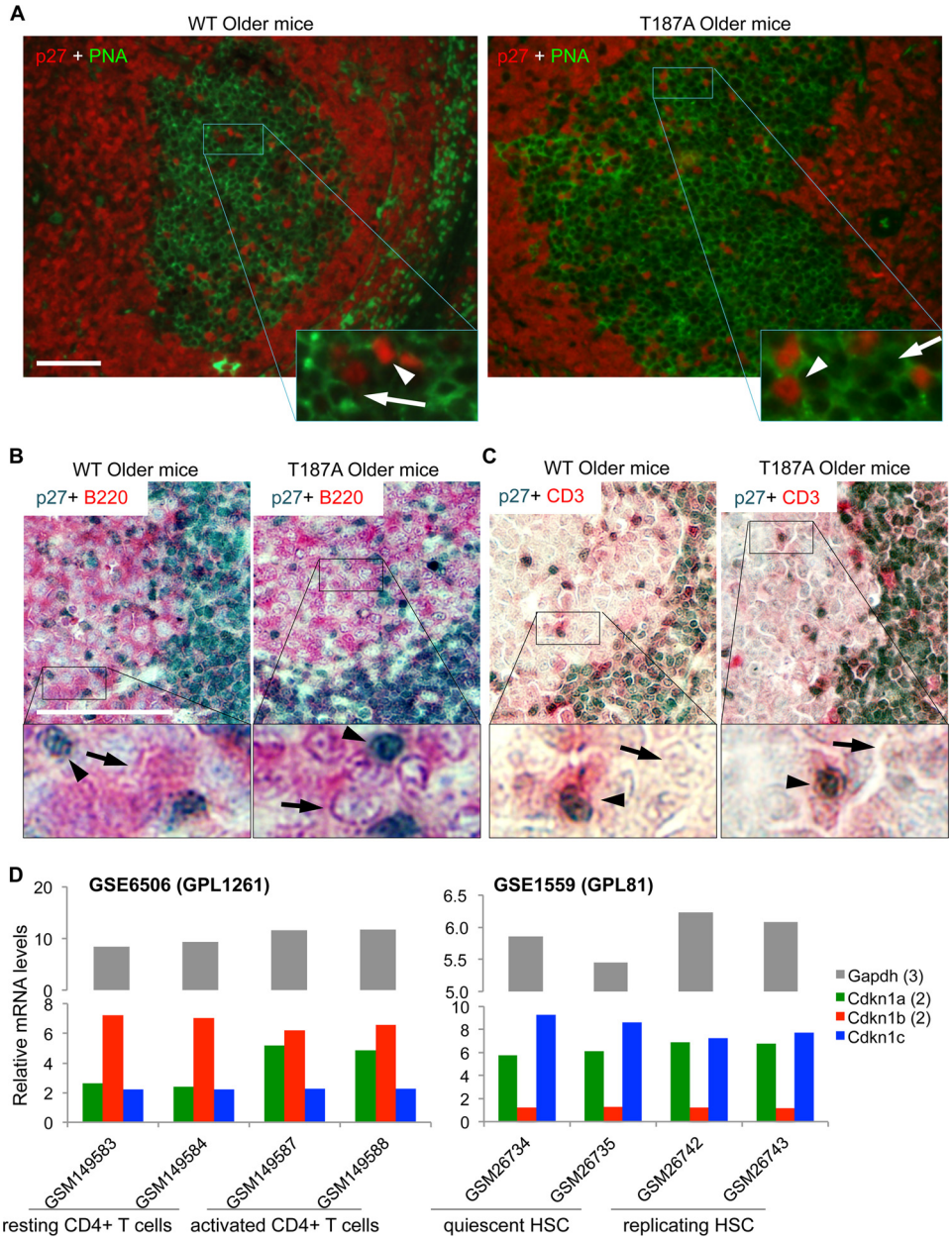

FIGURE 6. **p27 expression is dramatically reduced in GC B cells but maintained in GC T cells in older WT and older *p27*$^{T187A/T187A}$ mice at 10 days following SRBC immunization.** *A*, high magnification and red-green channel merge images of co-IF for p27 and PNA, as indicated, of representative GC, as marked. In enlarged areas, *white arrows* point to cells with membrane staining by PNA but negative for p27, while *white arrowheads* point to cells with positive staining for p27 without membrane PNA staining. *B*, two-color co-IHC for p27 (*dark blue*) and B cell marker B220 (*pink*), as marked, showing approximately one-quarter of a GC. *Black arrows* point to cells with positive membrane staining for B220 but negative for p27, while *black arrowheads* point to cells with positive p27 staining but negative for B220 membrane staining. *C*, same experiments as in *B*, except B220 antibody was replaced with CD3 antibody. *D*, in NCBI GEO database, gene expression profiles for naïve and activated CD4+ T cells (GSE6506) and quiescent and replicating HSC (GSE1559) were queried for expression of p21 (Cdkn1a, average of 2 probe sets), p27 (Cdkn1b, average of 2 probe sets), and p57 (Cdkn1c), as well as a housekeeping gene Gapdh (average of 3 probe sets). Sample records (GSMxxx) and experimental platforms (GPLxxx) are shown. Data in both datasets were normalized by GC-RMA, and two biological replicates were analyzed.

found three such datasets and queried them for expression of the three p27 family members including p21 (Cdkn1a), p27 (Cdkn1b), and p57 (Cdkn1c) together with a housekeeping gene *Gapdh*. As shown in Fig. 5*D*, p27 mRNA levels were reduced by 5.5 to 10.5-fold in GSE4142, 117 to 9.5-fold in GSE8906, or 4.7 to 10.6-fold in GSE23925 when naïve B cells

FIGURE 5. **p27 expression is reduced in GC in both older WT and older *p27*$^{T187A/T187A}$ mice.** Spleen samples were collected 10 days following SRBC immunization, and stained by IHC with anti-B220 (*A, a* and *e*), anti-CD3 (*B, a* and *e*), or anti-p27 (*C, a* and *e*). Co-IF was then performed with PNA and each of these three antibodies to identify areas of GC, pointed by *white arrows*, in stains by each of these three antibodies (*b,c,d* and *f,g,h panels*). Scale bars, 200 μm. *D*, three gene expression profile databases (NCBI GEO accession numbers, GSExxx, are as marked) were queried for expression of p27 family members p21 (Cdkn1a, average of 2 probe sets), p27 (Cdkn1b, average of 2 probe sets), and p57 (Cdkn1c), as well as a housekeeping gene Gapdh (average of 3 probe sets). Sample records (GSMxxx) obtained from purified naïve B cells and GC B cells are as marked. Accession numbers GPLxxx contain information on experimental platforms (Affymatrix microarrays). Data in GSE4142 were RMA (Robust Multi-array Average) normalized unlogged, and GSE23925 was normalized by RMA. GSE8906 contained raw data. Two to three biological replicates were analyzed.

were compared with GC B cells. In the same samples, p21 and p57, as well as Gapdh, mRNA levels showed no such reduction patterns.

These findings suggest the activation of a robust mechanism that inhibited p27 mRNA expression when naïve B cells are stimulated to enter GC to proliferate. The dramatic p27 mRNA down-regulation might have overridden any reduction in p27 protein degradation caused by p27T187A KI, resulting in dramatic p27 protein level reductions in GC B cells in both WT and $p27^{T187A/T187A}$ mice, as shown in Fig. 5*C*. With this line of reasoning, we conclude that the enhanced GC reaction in older T187A mice is not caused by p27T187A KI cell-autonomously in GC B cells.

GC T Cells Maintain p27 Protein Levels—Because GC B cells dramatically down-regulate both p27 mRNA and protein expression, any effects of the p27T187A KI on p27 protein degradation might be inconsequential in GC B cells. We reasoned that cells in GC that maintain p27 protein levels are more likely to be affected by p27T187A KI. Although B cells outnumber T cells within GC, the CD4+ helper T cells in GC play a critical role in all aspects of the GC response including its initiation, expansion, and termination (24). As such, we next focused our p27 protein expression study on GC T cells. High magnification images of p27 and PNA co-IF indeed revealed a number of p27-positive cells in GC (Fig. 6*A*), with the vast majority of the p27-positive cells stained negative for PNA (*white arrowheads*), indicating that they are not B cells.

To determine the lineage status of the p27 expressing cells in GC, we concurrently stained p27 with either B220 or CD3 in double IHC. Consistent with co-IF for p27 and PNA in Fig. 6*A*, p27 positive cells in GC are negative for B220 in co-IHC (Fig. 6*B*, *black arrowheads*), while most cells in GC show positive B220 membrane staining with negative p27 staining (*black arrows*). In contrast, p27 positive cells in GC are positive for CD3 in co-IHC while most cells in GC are negative for both p27 and CD3 (Fig. 6*C*, *black arrowheads* and *black arrows*, respectively). These findings demonstrate that, while GC B cells dramatically down regulate p27 protein expression, GC T cells maintain p27 protein expression. Based on the IHC technique, we could not demonstrate any difference in p27 protein levels between the WT and $p27^{T187A/T187A}$ GC T cells.

Rapid proliferation of GC B cells leading to the generation of GC in response to immunization by T cell dependent antigen is completely dependent on CD4+ T helper cells (29). Inhibition of T cell proliferation by transgenic expression of p27 in T cells (from the mouse *Lck* promoter) blocked spleen GC reactions (30). Decline in CD4+ T cell population with aging has been suggested as a cause for the decline in GC response to T cell-dependent antigen immunization in older WT mice (31, 32). And it is known that proliferation of splenic CD4+ T helper cells in response to stimulation by anti-TCR was significantly (80%) reduced by p27T187A KI (11).

Combining these previous knowledge with our current findings that GC B cells do not express p27 mRNA and protein but GC T cells maintain p27 protein expression led us to hypothesize that CD4+ T cells in young $p27^{T187A/T187A}$ mice might be more difficult to activate and therefore have undergone less accumulative proliferation to have conserved a larger proliferative reservoir to maintain robust GC responses in older $p27^{T187A/T187A}$ mice. This principle is well known in stem cell studies (33, 34). In adult mice, hematopoietic stem cells (HSCs) remain proliferative quiescence until stimulated to proliferate to replenish the lost cell population. In resemblance, naïve CD4+ T cells are resting until activated by antigen binding to TCR to expand and migrate to GC to play essential roles in establishing humoral immunity (35, 36). In fact, it was shown in 2007 that CD4+ T cell activation and HSC activation shared both up-regulated and down-regulated gene expression programs (37). To determine whether regulation of p27 mRNA expression is also similar between CD4+ T cell activation and HSC activation, we queried NCBI GEO databases as shown in Fig. 6*D*. In GSE6506 (37) mouse splenic CD4+ T cells were activated by Concanavalin A and, in GSE1559 (38), mouse HSCs were activated by administering 5-fluorouracil. We found that p27 mRNA levels were not reduced when naïve CD4+ T cells were activated, consistent with the presence of p27 positive T cells in GC (Fig. 6*C*). Interestingly, p27 mRNA levels were also not reduced when HSCs were activated to replicate. These findings add a further relatedness between the activation programs in naïve CD4+ T cells and adult HSCs. Lack of p27 mRNA down-regulation could provide an opportunity for p27 down-regulation by p27 protein degradation.

Spleen CD4+/CD8+ T Cell Ratios following SRBC Immunization Is Higher in Older $p27^{T187A/T187A}$ Mice than in Older WT Mice—Altered cell proliferation control may lead to changes in clonal expansion, differentiation, and cell death. As an indirect measurement of the impact of p27 T187A KI on lymphocyte population maintenance, we assessed the population size of total T and B cells (as T/B cell ratios), and CD4+ and CD8+ T cell subsets (as CD4+/CD8+ T cell ratios) in older mice. As shown in Fig. 7*A*, the T/B cell ratios were comparable between WT and $p27^{T187A/T187A}$ mice. Interestingly, the ratio of CD4+ helper T cells over CD8+ killer T was significantly higher in older $p27^{T187A/T187A}$ mice compared with older WT mice (Fig. 7*B*). This finding suggests that a more difficult-to-activate CD4+ T cell population in $p27^{T187A/T187A}$ mice (11) might have better maintained its population size in older age, and could explain how older $p27^{T187A/T187A}$ mice responded more robustly than older WT mice to SRBC immunization. To strengthen this finding, we further determined the CD4+/CD8+ T cell ratios inside CD3+ gate, and obtained similar results (Fig. 7*C*). We conclude that older $p27^{T187A/T187A}$ mice contained larger populations of CD4+ T cells during SRBC immunization, which, at least in part, enhanced GC B cell reaction.

DISCUSSION

Modeling Effects of Skp2/Cks1-p27T187p Interaction Inhibitors—Roles of p27 in proliferation related physiology have been well studied with loss-of-function approaches using p27 KO mice and p27 ck- mice. Since increasing p27 is an actively developing cancer therapy strategy, studying effects of p27 gain-of-function in proliferation related physiology would more directly facilitate cancer therapy development. In this regard, $p27^{T187A/T187A}$ mice are especially important since they model actions of an actively developing type of inhibitors that block p27T187p interaction with Skp2/Cks1 (see Introduction). Fur-

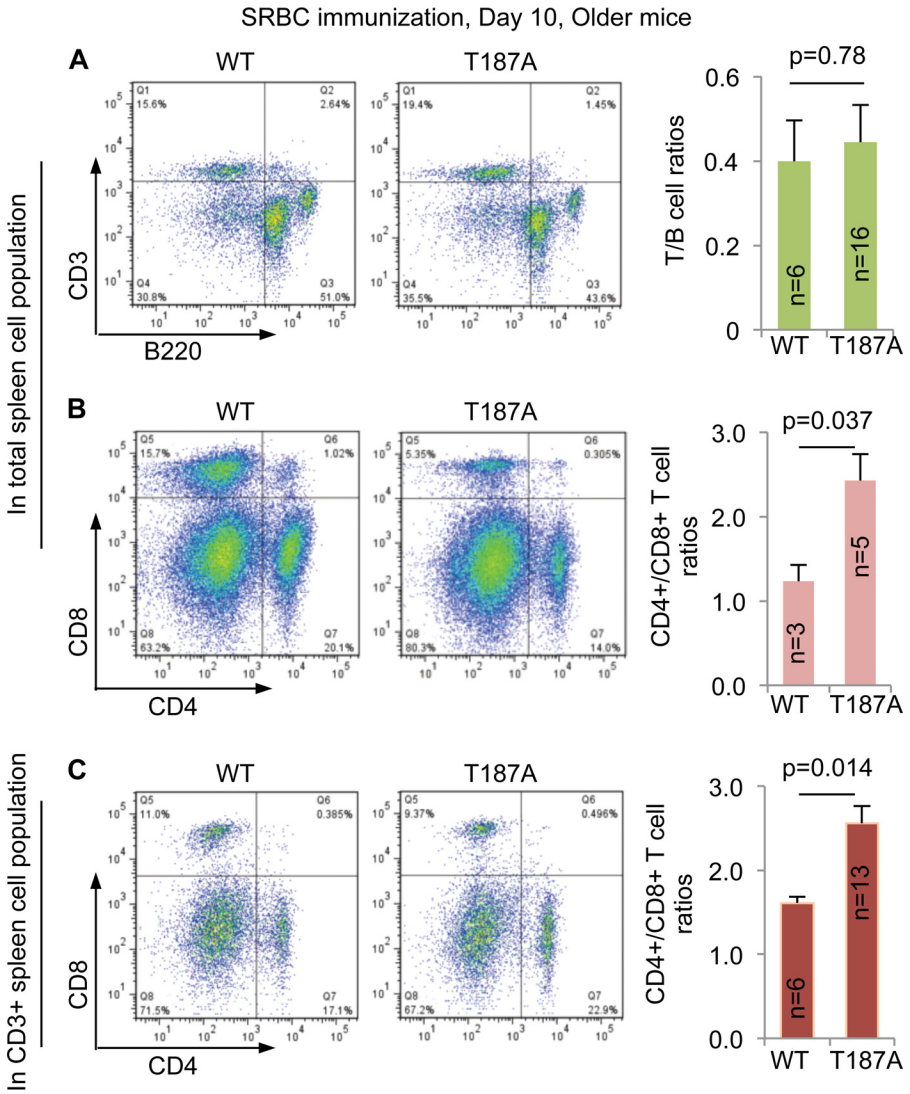

FIGURE 7. **CD4+/CD8+ T cell ratios are higher in older $p27^{T187A/T187A}$ mice than in older WT mice at 10 days following SRBC immunization.** *A*, representative FACS profiles of spleen cell suspensions following CD3 and B220 double staining and quantifications. *B*, FACS profiles following CD4 and CD8 double staining of total spleen cell suspension and quantifications. *C*, FACS profiles following CD4 and CD8 double staining of CD3+ cells in spleen cell suspension and quantifications. *p* values are from two-tailed Student's *t* tests, and error bars represent S.E.

ther, $p27^{T187A/T187A}$ mice do not accumulate p27 protein in quiescent tissues and their lack of overt defects already demonstrated that inhibitors of p27T187p interaction with Skp2/Cks1 should be harmless to normal physiology. Remarkably, since its generation and first characterization in 2001 (11), studies of $p27^{T187A/T187A}$ mice have revealed few physiological phenotypes including tumorigenesis (see Introduction). Our study now reveal that fully penetrant pituitary tumorigenesis in $Rb1^{+/-}$ mice is fully blocked in $Rb1^{+/-}$;$p27^{T187A/T187A}$ mice, identifying $Rb1^{+/-}$ mice as the preclinical tumor model against which inhibitors of p27T187p interaction with Skp2/Cks1 can be definitively compared.

p27T187A KI models the most potent inhibitors of p27T187p-Skp2/Cks1 interaction and, therefore, can be an impossible match for inhibitor candidates. On the other hand, inhibitors of p27T187p-Skp2/Cks1 interaction may also block interaction of Skp2-Cks1 to p27 family members p21 and any unknown substrates of $SCF^{Skp2/Cks1}$, potentially inhibiting pituitary tumorigenesis in $Rb1^{+/-}$ mice through mechanisms other than stabilizing p27. More sophisticated preclinical mouse tumor models may be desired to improve on these aspects of inhibitor testing using $Rb1^{+/-}$ mice.

Mechanisms of Tumor Blocking in $Rb1^{+/-}$;$p27^{T187A/T187A}$ Mice—In our previous studies, we induced mouse pituitary IL tumors by artificial deletion of *Rb1* in all melanotrophs and POMC-Cre;$Rb1^{lox/lox}$ mice developed pituitary tumors across the entire IL. POMC-Cre;$Rb1^{lox/lox}$;$p27^{T187A/T187A}$ mice produced greatly thinned pituitary IL with apoptosis (19). In this artificial setting, p27T187A KI resulted in synthetic lethality with *Rb1* deletion by further activating E2F1 (39). Our current finding documents a tumor suppressive role of p27T187A KI in a physiological "two hit" setting. Whether this block was achieved by promoting apoptosis or inhibiting proliferation is difficult to determine in the "two hit" setting. It is however likely that the observed blocking to pituitary tumorigenesis by two hit *Rb1* loss does not require significant accumulation of p27, since p27 IHC showed similarly low levels of p27 in WT, $p27^{T187A/T187A}$, and $Rb1^{+/-}$;$p27^{T187A/T187A}$ IL (Fig. 1*B*).

It is notable that, p27T187A KI showed little antitumor effects in lung tumorigenesis by oncogenic activation of endogenous *Kras* (14), another tumor model in a physiological setting. Since p27 mRNA levels were significantly reduced in this lung tumor model (14), the lack of an antitumor phenotype demonstrates that the inhibitory effects of p27T187A KI on p27 protein degradation might only be relevant when p27 protein levels were reduced primarily by enhanced protein degradation. Differences in oncogenic mechanisms by two hit loss of *Rb1* in melanotrophs and by activation of endogenous *Kras* in lung may also determine whether p27T187A KI is effective. Now that the "positive control" is available (that $Rb1^{+/-}$; $p27^{T187A/T187A}$ mice do not develop pituitary tumors), testing antitumor effects of p27T187A KI in other physiological mouse tumor models will be more informative.

How Does p27T187A KI Maintain Robust Antibody Response to SRBC Immunization?—While blocking pituitary tumorigenesis by "two hit" loss of *Rb1* identifies a sought-after role for an anticipated effect, enhancing GC B cell expansion leading to improved antigen specific humoral immunity in older mice is opposite to our anticipation. This unexpected finding has the potential to address another important medical issue: improve vaccination efficacy in the elderly. Vaccination efficacy depends on long lived plasma cells and memory B cells, both of them produced by the GC reaction following immunization. Both B and T cell repertoires experience age-associated impairment in mice and humans. In co-transfer experiments testing different combination of old and young B and T cells, it was observed that the age-related GC impairment mainly engrafts with old T cells instead of old B cells (32, 40). More recent studies have revealed multiple, age-associated molecular changes in the follicular T helper cell lineage (Tfh cells, which are CD4+ T cells in GC) (26). Our findings have now implicated the regulation of p27 protein stability in these aspects.

We suggest that ubiquitination of p27T187p by $SCF^{Skp2/Cks1}$ in CD4+ T cells may have set a threshold for their activation at a level that could lead these cells to proliferate in young age to the extent that compromises their proliferation in older age. Indeed, there were more GCs in a given area of the spleen section in older $p27^{T187A/T187A}$ mice than older WT mice (Fig. 4*B*), suggesting increased availability of cognitive T cells to SRBC-reactive B cells to initiate the GC response in the mutant mice. In other words, the efficiency of T cell priming, which is normally reduced with aging (26, 29), was maintained by the expression of the p27T187A protein. In humans, reduced antibody response to vaccination correlates with reduced frequency of naïve T cells (41). Thus, it is possible that a stabilized p27 protein and the consequent reduced cell cycle activity upon antigen stimulation (11) preserved more proliferation potential of the naïve CD4+ T cell pool, while this pool is diminished with aging in WT mice. This notion is supported by our observation that older $p27^{T187A/T187A}$ mice had a higher CD4+/CD8+ T cell ratio relative to older WT mice (Fig. 7).

The second aspect of the observed enhanced GC phenotype is that individual GCs formed in older $p27^{T187A/T187A}$ mice was 77% larger on average than those in older WT mice (Fig. 4*C*), indicating that more mitogenic signals were provided by Tfh in GC to the GC B cells, which is another aspect of T cell function known to deteriorate with aging (26, 29). While detailed molecular mechanisms linking a stabilized p27 protein to enhanced B cell help function of GC T cells await future studies, it is worth noting that a recent study has correlated reduced proliferation of Tfh cells to their enhanced B cell help function (42).

In summary, our study have provided evidence that targeting p27T187 phosphorylation-dependent ubiquitination by $SCF^{Skp2/Cks1}$ could be very effective against specific types of cancer (43) and have suggested strategies to better understand, and potentially leading to methods to prevent, the decline of humoral immunity in the elderly (26).

Acknowledgments—We thank Dr. James Roberts for providing the p27T187A KI mice, Hong Zhang and Drs. Yong Chen and Giorgio Cattoretti for valuable suggestions in spleen IF and IHC, and Dr. Herbert Morse III for assistance with histopathological evaluation of the spleen sections. Albert Einstein Comprehensive Cancer Research Center (5P30CA13330) and Liver Research Center (5P30DK061153) provided core facility support.

REFERENCES

1. Nakayama, K., Ishida, N., Shirane, M., Inomata, A., Inoue, T., Shishido, N., Horii, I., Loh, D. Y., and Nakayama, K.-i. (1996) Mice lacking p27Kip1 display increased body size, multiple organ hyperplasia, retinal dysplasia, and pituitary tumors. *Cell* **85,** 707–720
2. Fero, M. L., Rivkin, M., Tasch, M., Porter, P., Carow, C. E., Firpo, E., Polyak, K., Tsai, L.-H., Broudy, V., Perlmutter, R. M., Kaushansky, K., and Roberts, J. M. (1996) A syndrome of multiorgan hyperplasia with features of gigantism, tumorigenesis, and female sterility in p27Kip1-deficient mice. *Cell* **85,** 733–744
3. Kiyokawa, H., Kineman, R. D., Manova-Todorova, K., Soares, V. C., Hoffman, E. S., Ono, M., Khanam, D., Hayday, A. C., Frohman, L. A., and Koff, A. (1996) Enhanced growth of mice lacking the cyclin-dependent kinase inhibitor function of p27Kip1. *Cell* **85,** 721–732
4. Besson, A., Gurian-West, M., Chen, X., Kelly-Spratt, K. S., Kemp, C. J., and Roberts, J. M. (2006) A pathway in quiescent cells that controls p27Kip1 stability, subcellular localization, and tumor suppression. *Genes Dev.* **20,** 47–64
5. Bassermann, F., Eichner, R., and Pagano, M. (2014) The ubiquitin proteasome system - implications for cell cycle control and the targeted treatment of cancer. *Biochim. Biophys. Acta* **1843,** 150–162
6. Vlach, J., Hennecke, S., and Amati, B. (1997) Phosphorylation-dependent degradation of the cyclin-dependent kinase inhibitor p27. *EMBO J.* **16,** 5334–5344
7. Montagnoli, A., Fiore, F., Eytan, E., Carrano, A. C., Draetta, G. F., Hershko, A., and Pagano, M. (1999) Ubiquitination of p27 is regulated by Cdk-dependent phosphorylation and trimeric complex formation. *Genes Dev.* **13,** 1181–1189
8. Ganoth, D., Bornstein, G., Ko, T. K., Larsen, B., Tyers, M., Pagano, M., and Hershko, A. (2001) The cell-cycle regulatory protein Cks1 is required for SCF(Skp2)-mediated ubiquitinylation of p27. *Nat. Cell Biol.* **3,** 321–324
9. Spruck, C., Strohmaier, H., Watson, M., Smith, A. P. L., Ryan, A., Krek, W., and Reed, S. I. (2001) A CDK-independent function of mammalian Cks1: targeting of SCF^{Skp2} to the CDK inhibitor $p27^{Kip1}$. *Mol. Cell* **7,** 639–650
10. Hao, B., Zheng, N., Schulman, B. A., Wu, G., Miller, J. J., Pagano, M., and Pavletich, N. P. (2005) Structural basis of the Cks1-dependent recognition of p27(Kip1) by the SCF(Skp2) ubiquitin ligase. *Mol. Cell* **20,** 9–19
11. Malek, N. P., Sundberg, H., McGrew, S., Nakayama, K., Kyriakides, T. R., and Roberts, J. M. (2001) A mouse knock-in model exposes sequential proteolytic pathways that regulate p27Kip1 in G1 and S phase. *Nature* **413,** 323–327
12. Kossatz, U., Dietrich, N., Zender, L., Buer, J., Manns, M. P., and Malek, N. P. (2004) Skp2-dependent degradation of p27kip1 is essential for cell cycle progression. *Genes Dev.* **18,** 2602–2607

13. Sanz-González, S. M., Melero-Fernández de Mera, R., Malek, N. P., and Andrés, V. (2006) Atheroma development in apolipoprotein E-null mice is not regulated by phosphorylation of p27(Kip1) on threonine 187. *J. Cell. Biochem.* **97,** 735–743
14. Timmerbeul, I., Garrett-Engele, C. M., Kossatz, U., Chen, X., Firpo, E., Grünwald, V., Kamino, K., Wilkens, L., Lehmann, U., Buer, J., Geffers, R., Kubicka, S., Manns, M. P., Porter, P. L., Roberts, J. M., and Malek, N. P. (2006) Testing the importance of p27 degradation by the SCFskp2 pathway in murine models of lung and colon cancer. *Proc. Natl. Acad. Sci. U.S.A.* **103,** 14009–14014
15. Wu, L., Grigoryan, A. V., Li, Y., Hao, B., Pagano, M., and Cardozo, T. J. (2012) Specific small molecule inhibitors of Skp2-mediated p27 degradation. *Chem. Biol.* **19,** 1515–1524
16. Ungermannova, D., Lee, J., Zhang, G., Dallmann, H. G., McHenry, C. S., and Liu, X. (2013) High-throughput screening AlphaScreen assay for identification of small-molecule inhibitors of ubiquitin E3 ligase SCF-Skp2-Cks1. *J. Biomol. Screen.* **18,** 910–920
17. Ooi, L. C., Watanabe, N., Futamura, Y., Sulaiman, S. F., Darah, I., and Osada, H. (2013) Identification of small molecule inhibitors of p27(Kip1) ubiquitination by high-throughput screening. *Cancer Science* **104,** 1461–1467
18. Victora, G. D. (2014) SnapShot: The Germinal Center Reaction. *Cell* **159,** 700–700.e701
19. Wang, H., Bauzon, F., Ji, P., Xu, X., Sun, D., Locker, J., Sellers, R. S., Nakayama, K., Nakayama, K. I., Cobrinik, D., and Zhu, L. (2010) Skp2 is required for survival of aberrantly proliferating Rb1-deficient cells and for tumorigenesis in Rb1+/- mice. *Nat. Genet.* **42,** 83–88
20. Peled, J. U., Yu, J. J., Venkatesh, J., Bi, E., Ding, B. B., Krupski-Downs, M., Shaknovich, R., Sicinski, P., Diamond, B., Scharff, M. D., and Ye, B. H. (2010) Requirement for cyclin D3 in germinal center formation and function. *Cell Res.* **20,** 631–646
21. Jacks, T., Fazeli, A., Schmitt, E. M., Bronson, R. T., Goodell, M. A., and Weinberg, R. A. (1992) Effects of an Rb mutation in the mouse. *Nature* **359,** 295–300
22. Zhao, H., Bauzon, F., Fu, H., Lu, Z., Cui, J., Nakayama, K., Nakayama, K. I., Locker, J., and Zhu, L. (2013) Skp2 Deletion Unmasks a p27 Safeguard that Blocks Tumorigenesis in the Absence of pRb and p53 Tumor Suppressors. *Cancer Cell* **24,** 645–659
23. MacLennan, I. C. (1994) Germinal centers. *Annu. Rev. Immunol.* **12,** 117–139
24. Crotty, S. (2011) Follicular helper CD4 T cells (TFH). *Annu. Rev. Immunol.* **29,** 621–663
25. Béguelin, W., Popovic, R., Teater, M., Jiang, Y., Bunting, K. L., Rosen, M., Shen, H., Yang, S. N., Wang, L., Ezponda, T., Martinez-Garcia, E., Zhang, H., Zheng, Y., Verma, S. K., McCabe, M. T., Ott, H. M., Van Aller, G. S., Kruger, R. G., Liu, Y., McHugh, C. F., Scott, D. W., Chung, Y. R., Kelleher, N., Shaknovich, R., Creasy, C. L., Gascoyne, R. D., Wong, K. K., Cerchietti, L., Levine, R. L., Abdel-Wahab, O., Licht, J. D., Elemento, O., and Melnick, A. M. (2013) EZH2 is required for germinal center formation and somatic EZH2 mutations promote lymphoid transformation. *Cancer Cell* **23,** 677–692
26. Linterman, M. A. (2014) How T follicular helper cells and the germinal centre response change with age. *Immunol. Cell Biol.* **92,** 72–79
27. Mountz, J. D., Wang, J. H., Xie, S., and Hsu, H. C. (2011) Cytokine regulation of B-cell migratory behavior favors formation of germinal centers in autoimmune disease. *Discovery Medicine* **11,** 76–85
28. Bronte, V., and Pittet, M. J. (2013) The spleen in local and systemic regulation of immunity. *Immunity* **39,** 806–818
29. Foy, T. M., Aruffo, A., Bajorath, J., Buhlmann, J. E., and Noelle, R. J. (1996) Immune regulation by CD40 and its ligand GP39. *Annu. Rev. Immunol.* **14,** 591–617
30. Tsukiyama, T., Ishida, N., Shirane, M., Minamishima, Y. A., Hatakeyama, S., Kitagawa, M., Nakayama, K., and Nakayama, K. (2001) Down-regulation of p27Kip1 expression is required for development and function of T cells. *J. Immunol.* **166,** 304–312
31. Callahan, J. E., Kappler, J. W., and Marrack, P. (1993) Unexpected expansions of CD8-bearing cells in old mice. *J. Immunol.* **151,** 6657–6669
32. Eaton, S. M., Burns, E. M., Kusser, K., Randall, T. D., and Haynes, L. (2004) Age-related defects in CD4 T cell cognate helper function lead to reductions in humoral responses. *J. Exp. Med.* **200,** 1613–1622
33. Liu, L., Cheung, T. H., Charville, G. W., Hurgo, B. M., Leavitt, T., Shih, J., Brunet, A., and Rando, T. A. (2013) Chromatin modifications as determinants of muscle stem cell quiescence and chronological aging. *Cell Reports* **4,** 189–204
34. Cheung, T. H., and Rando, T. A. (2013) Molecular regulation of stem cell quiescence. *Nat. Rev. Mol. Cell Biol.* **14,** 329–340
35. Shulman, Z., Gitlin, A. D., Targ, S., Jankovic, M., Pasqual, G., Nussenzweig, M. C., and Victora, G. D. (2013) T follicular helper cell dynamics in germinal centers. *Science* **341,** 673–677
36. Gitlin, A. D., Shulman, Z., and Nussenzweig, M. C. (2014) Clonal selection in the germinal centre by regulated proliferation and hypermutation. *Nature* **509,** 637–640
37. Chambers, S. M., Boles, N. C., Lin, K. Y., Tierney, M. P., Bowman, T. V., Bradfute, S. B., Chen, A. J., Merchant, A. A., Sirin, O., Weksberg, D. C., Merchant, M. G., Fisk, C. J., Shaw, C. A., and Goodell, M. A. (2007) Hematopoietic fingerprints: an expression database of stem cells and their progeny. *Cell Stem Cell* **1,** 578–591
38. Venezia, T. A., Merchant, A. A., Ramos, C. A., Whitehouse, N. L., Young, A. S., Shaw, C. A., and Goodell, M. A. (2004) Molecular signatures of proliferation and quiescence in hematopoietic stem cells. *PLoS Biology* **2,** e301
39. Lu, Z., Bauzon, F., Fu, H., Cui, J., Zhao, H., Nakayama, K., Nakayama, K. I., and Zhu, L. (2014) Skp2 suppresses apoptosis in Rb1-deficient tumours by limiting E2F1 activity. *Nat. Commun.* **5,** 3463
40. Yang, X., Stedra, J., and Cerny, J. (1996) Relative contribution of T and B cells to hypermutation and selection of the antibody repertoire in germinal centers of aged mice. *J. Exp. Med.* **183,** 959–970
41. Looney, R. J., Hasan, M. S., Coffin, D., Campbell, D., Falsey, A. R., Kolassa, J., Agosti, J. M., Abraham, G. N., and Evans, T. G. (2001) Hepatitis B immunization of healthy elderly adults: relationship between naïve CD4+ T cells and primary immune response and evaluation of GM-CSF as an adjuvant. *J. Clin. Immunol.* **21,** 30–36
42. Good-Jacobson, K. L., Szumilas, C. G., Chen, L., Sharpe, A. H., Tomayko, M. M., and Shlomchik, M. J. (2010) PD-1 regulates germinal center B cell survival and the formation and affinity of long-lived plasma cells. *Nat. Immunol.* **11,** 535–542
43. Zhu, L., Lu, Z., and Zhao, H. (2014) Antitumor mechanisms when pRb and p53 are genetically inactivated. *Oncogene* 10.1038/onc.2014.399

Substituting Threonine 187 with Alanine in p27Kip1 Prevents Pituitary Tumorigenesis by Two-Hit Loss of *Rb1* and Enhances Humoral Immunity in Old Age

Hongling Zhao, Frederick Bauzon, Enguang Bi, J. Jessica Yu, Hao Fu, Zhonglei Lu, Jinhua Cui, Hyungjun Jeon, Xingxing Zang, B. Hilda Ye and Liang Zhu

J. Biol. Chem. 2015, 290:5797-5809.
doi: 10.1074/jbc.M114.625350 originally published online January 12, 2015